Journal of Archaeological Science 38 (2011) 2141–2154

Contents lists available at ScienceDirect

Journal of Archaeological Science

journal homepage: http://www.elsevier.com/locate/jas

Airborne lidar survey of irrigated agricultural landscapes: an application of the slope contrast method

Mark D. McCoy [a,*], Gregory P. Asner [b], Michael W. Graves [c]

[a] Department of Anthropology, University of Otago, P.O. Box 56, Dunedin 9054, New Zealand
[b] Carnegie Institution for Science, USA
[c] University of New Mexico, Department of Anthropology, USA

ARTICLE INFO

Article history:
Received 22 December 2010
Received in revised form
24 February 2011
Accepted 25 February 2011

Keywords:
Lidar
GIS
Remote sensing
Landscape archaeology
Irrigation
Hawai'i

ABSTRACT

Irrigated agriculture was central to the economies of many of the world's best known complex societies. New high-resolution digital elevation models (DEM) derived from remotely sensed lidar data give archaeologists the opportunity to study field systems at a scale not previously possible. Here we describe a method called slope contrast mapping that takes advantage of the dissimilarity between artificial and natural slopes to identify and map discrete features. We use this relatively simple method in our own research to identify complexes of agricultural terraces in the North Kohala district, Hawai'i Island. It has also proved useful for mapping the natural landscape, specifically the extent of flat land between valleys suited for irrigated agriculture.

1. Introduction

Airborne lidar (light detection and ranging) has proven its utility for remote sensing in archaeology (Bewley et al., 2005; Challis, 2006; Challis and Howard, 2006; Challis et al., 2008; Crutchley, 2006; Harmon et al., 2006; Rowlands and Sarris, 2007; Lasaponara et al., 2010; McCoy and Ladefoged, 2009; Millard et al., 2009; Parcak, 2009), especially for mapping archaeological features in forested areas (Chase et al., 2010, 2011; Crow et al., 2007; Devereux et al., 2005; Doneus et al., 2008; Gallagher and Josephs, 2008), but also natural features relevant for archaeological research (Brown, 2008; Carey et al., 2006; Challis et al., 2011). At present, "applications of lidar still face challenges, especially in defining practical processing protocols" (Campbell, 2007:p. 249).

Lidar mapping typically relies on displaying high-resolution, digital elevation models (DEM), also known as digital terrain models (DTM), using two GIS functions: hillshade and three dimensional (3D) display. The 'hillshade' operation uses grayscale shading effects that mimic natural shadows based on specified height (altitude) and direction of light source (azimuth). Alternatively, one can choose to display a lidar DEM in 3D where the shape and heights of features can quite literally stand out from the background. Recent innovations in lidar interpretation do not rely on display manipulation and instead use advanced methods of filtering data to identify anomalies (Coluzzia et al., 2011; Doneus et al., 2008; Gallagher and Josephs, 2008; Hesse, 2010), or a derived value (e.g., sky-view factor, Kokalj et al., 2011). While the specific protocols for these methods vary, advanced methods essentially use elevation data to discriminated features built above or below the expected trend in the natural ground surface.

We describe an additional application for deriving cultural features from lidar DEM called slope contrast mapping. Slope contrast mapping takes advantage of marked changes in elevation to help identify and record archaeological features. Slope is first calculated and then classified in a raster (grid) surface as flat, low, or high. This raster is then vectorized into polygons representing micro-topographical regions that can be used to easily distinguish certain types of construction forms from the natural landscape, specifically artificially flat surfaces and steep banks created by cut and fill.

Slope contrast mapping is used here to identify groups of agricultural terraces in North Kohala district of Hawai'i Island. This same GIS layer is also used to identify flat-to-low slope areas between drainages, also known as tableland, where irrigation could have been expanded. Together, the archaeological and natural features identified give us a remarkable new picture of the peak amount of land under production in the study area and, in turn, provide insight into larger economic and political changes in pre-European contact Hawaiian society.

* Corresponding author. Tel.: +64 3 479 8748; fax: +64 3 479 9095.
E-mail address: mark.mccoy@otago.ac.nz (M.D. McCoy).

0305-4403/$ – see front matter © 2011 Elsevier Ltd. All rights reserved.
doi:10.1016/j.jas.2011.02.033

2. Background

2.1. The study area: windward North Kohala, Hawai'i Island

The transformation of the Hawaiian Islands from a pristine natural landscape to the massive anthropogenic patchwork of cultivated agricultural fields that marveled visitors in the late 18th century occurred over a period of no more than 1000 years beginning around A.D. 800–1000 (Kirch and McCoy, 2007). Over that time period the population of the archipelago grew from a few hundred people to a society of hundreds of thousands of people divided into polities in which a hierarchy of elites managed and collected taxes and tribute in the form of agricultural produce, or what is sometimes called surplus wealth. Kirch (1994) and others have contrasted territories that depended upon 'wet' and 'dry' environments arguing that the higher natural productivity of irrigated 'wet' agricultural systems provided less motivation for expansionist warfare when compared to non-irrigated 'dry' agricultural production systems (Fig. 1). Here, irrigated farming generally refers to the cultivation of taro (*Colocasia esculenta*) in pondfields where water is impounded in much the same way as rice paddies. Non-irrigated fields relied on rainfall alone and included a wider variety of crops including the staples sweet potatoes (*Ipomoea batatas*) and yams (*Dioscorea* spp.). For archaeologists it is critically important to determine the type and amount of agricultural lands within different Hawaiian districts as a first step to reconstructing the larger political economy, and the development of archaic states (Kirch, 2010).

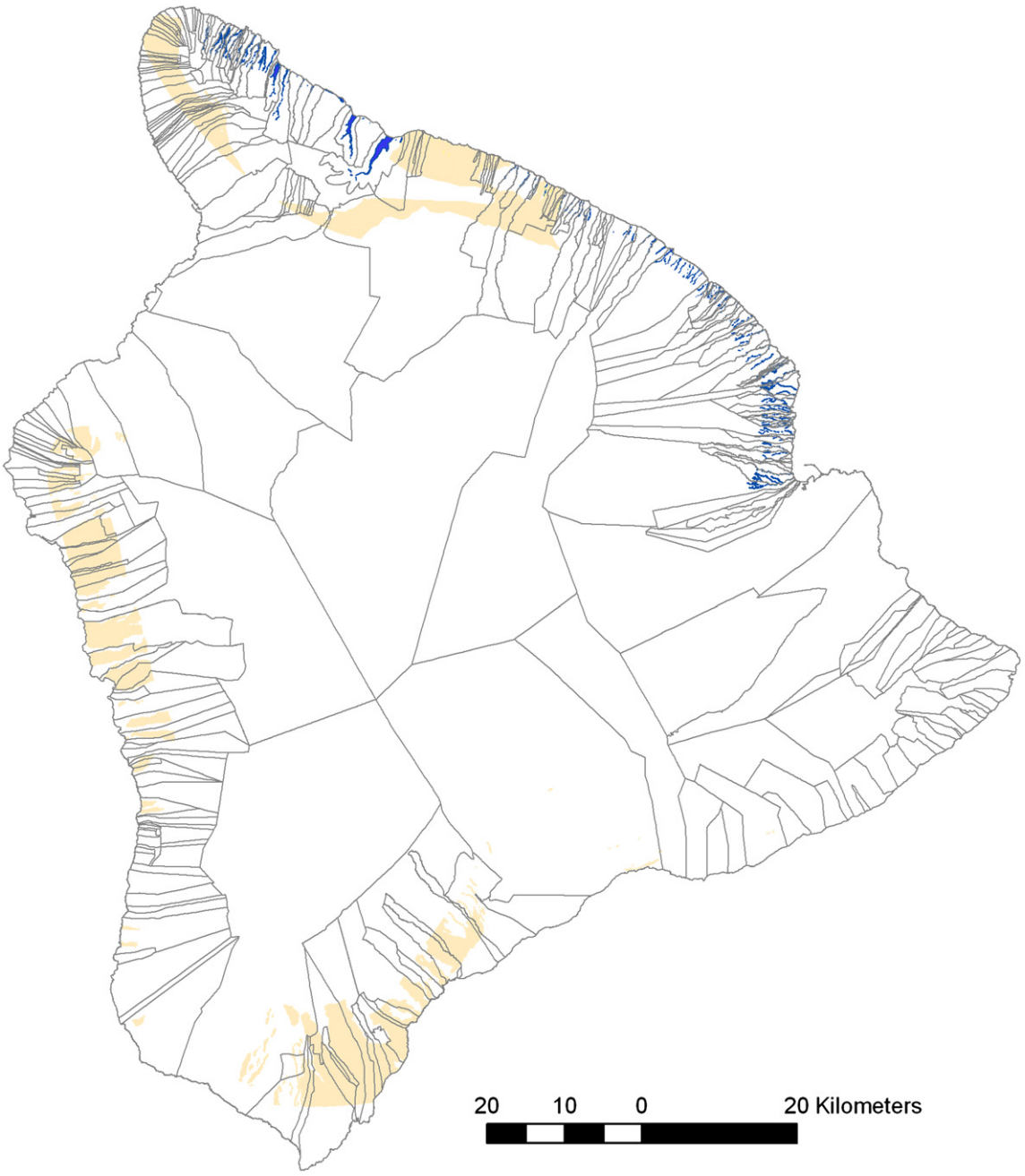

Fig. 1. Major Irrigated (blue) and Non-Irrigated Rain-fed Farming (yellow) Areas on Hawai'i Island (after Ladefoged et al., 2009). The North Kohala District, Hawai'i Island is located on the northernmost tip of the island. (For interpretation of the references to color in this figure legend, the reader is referred to the web version of this article.)

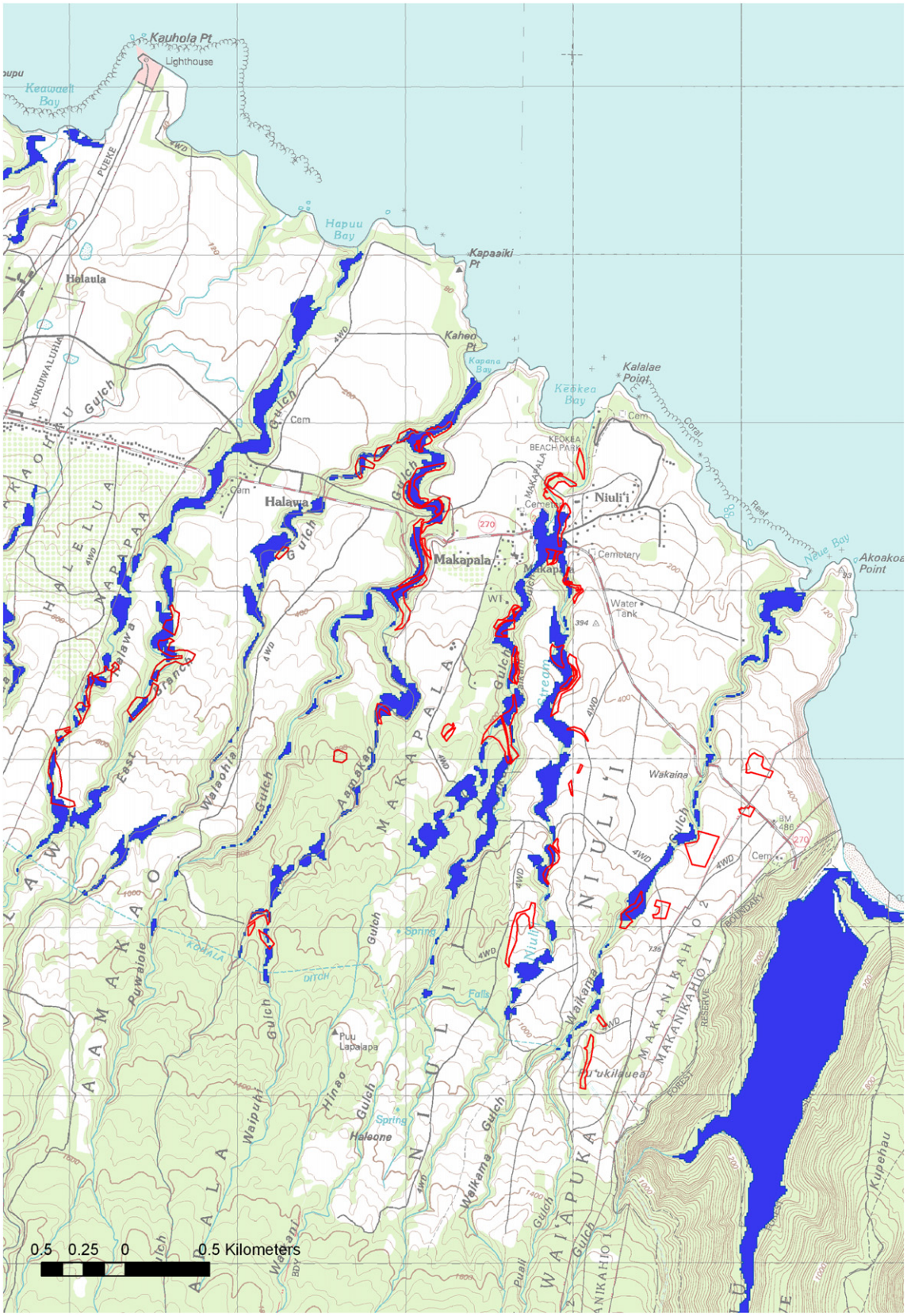

Fig. 2. Study Area: Windward North Kohala District, Hawai'i Island. This map shows maximum extent of irrigated agriculture predicted in a GIS model (Ladefoged et al., 2009) and known locations of irrigated farming at circa 1904–1935 (see McCoy and Graves, 2010). The larger Pololu Valley east of the study area is shown for size comparison.

Our research has focused on irrigated field system in the North Kohala district, Hawai'i Island (Fig. 2; McCoy and Graves, 2007, 2008, 2010). Located on the eastern flanks of the Kohala Mountains, the study area is comprised of a series of small valleys, or gulches, separated by narrow stretches of relative flat land, called tableland. Constant tradewinds ensure high rainfall and there is good evidence of irrigated farming at the base of these small valleys from the coast to far inland. However, estimates of the maximum area under production within valley bottoms have varied widely. Earle (1980, 2002) described this as a minor area for irrigated farming and gives a relatively low figure based on the distribution of features found on survey in neighboring valleys (Pololu, Honokane). A recent GIS model by Ladefoged et al. (2009) puts the figure much higher, suggesting that the environmental conditions are right for as much as 94 ha of irrigated valley agriculture. We have also made a minimum estimate of 32 ha small valley fields based on turn of the century maps however until now we have reserved judgment on the absolute total due to a lack of complete survey or historic information (estimate including tableland fields, 42.1 ha, McCoy and Graves, 2010:Table 2).

Further complicating the estimate of irrigated lands, our excavations have confirmed that Hawaiians used canals to carry water out of drainages to expand irrigated gardens to include adjacent tableland (McCoy and Graves, 2010). However, commercial sugarcane farming has nearly completely destroyed any direct evidence of this tableland agriculture. Moreover, the area's tableland and complex network of small valleys are poorly represented on modern maps, especially the critical division between the tableland and the top of valley slopes. This makes it nearly impossible to estimate the total tableland adjacent to valley fields that might have been targeted for expansion.

2.2. Environmental and technological limitations to agriculture in windward Kohala

The study area is made up of four drainage systems with watersheds connected by a complex network streams that start at the crest line of the Kohala Mountains and flow down to the Pacific Ocean (Fig. 3). Rainfall within these watersheds is high, ranging from 1000 to +3000 mm, well above the ideal range for crops like sweet potatoes but sufficient to grow taro without the addition of

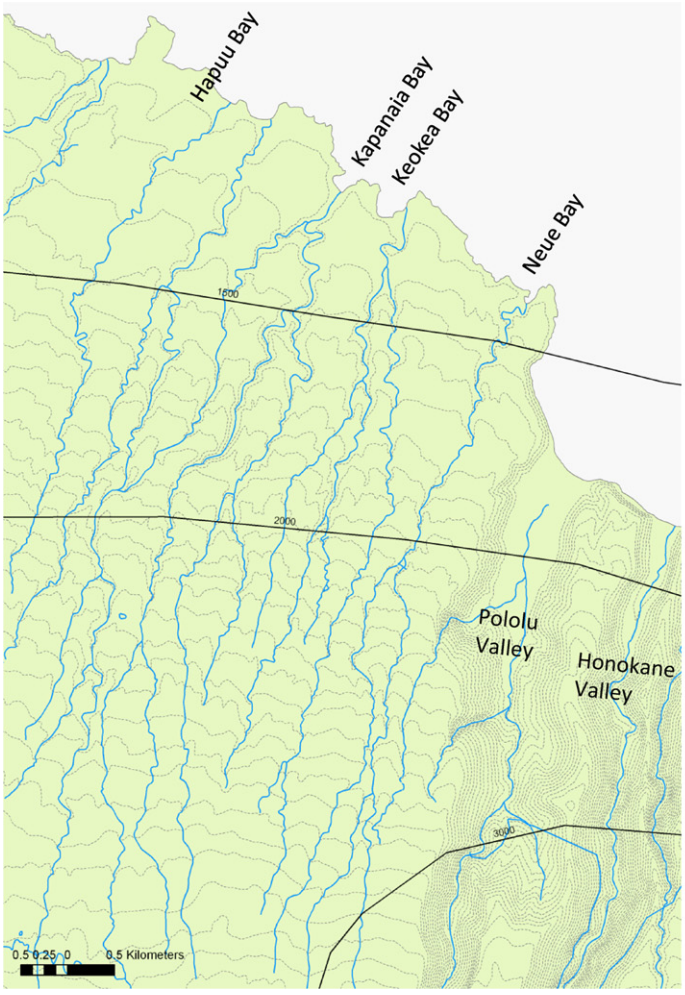

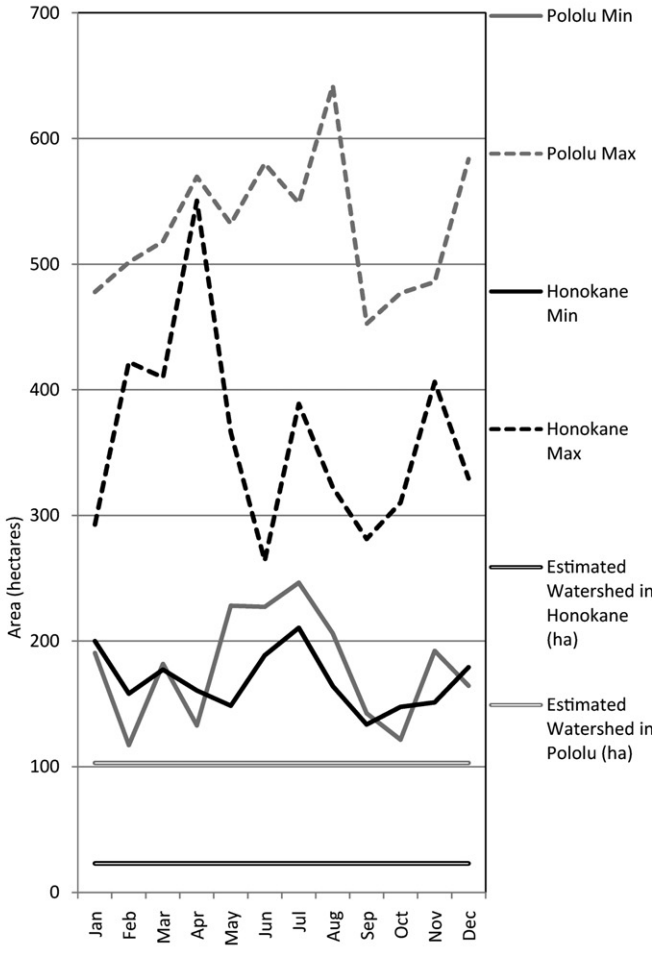

Fig. 3. Hydrology of North Kohala, Hawai'i. On the left, note the contrast between the easily definable watersheds of Pololu and Honokane Valleys as compared with small valley drainages in the study area where it is unclear which land is valley bottom, slope, or flat tableland between drainages. On the right, peak and minimum monthly average flows (USGS Stations: 16751000, 16747500) for Pololu and Honokane are expressed in terms of the amount of area that flow levels could have supported at the Hawaiian Legal Requirement of 280,000 L/ha/day. When compared with the total watershed it appears that there was sufficient water for irrigation on a massive scale. Source: http://waterdata.usgs.gov/hi/nwis/monthly. Raw flow values were converted from cubic feet per second.

irrigation water. Unfortunately, historic modification to vegetation and diversion of water for commercial agriculture make direct measurements of flow in these perennial streams unlikely to reflect pre-European contact levels. However, data from neighboring valleys, Pololu and Honokane, give us an idea of the range of discharge volume.

The critical factor for irrigated taro is maintaining consistent flow over the growing period. Year-round harvesting is possible if steady flow can be maintained at 280,000 L per ha per day (also known as the Hawaiian Legal Requirement). If we take the lowest monthly averages of flow from stream monitoring stations, we find that even at their weakest levels Pololu and Honokane Valley

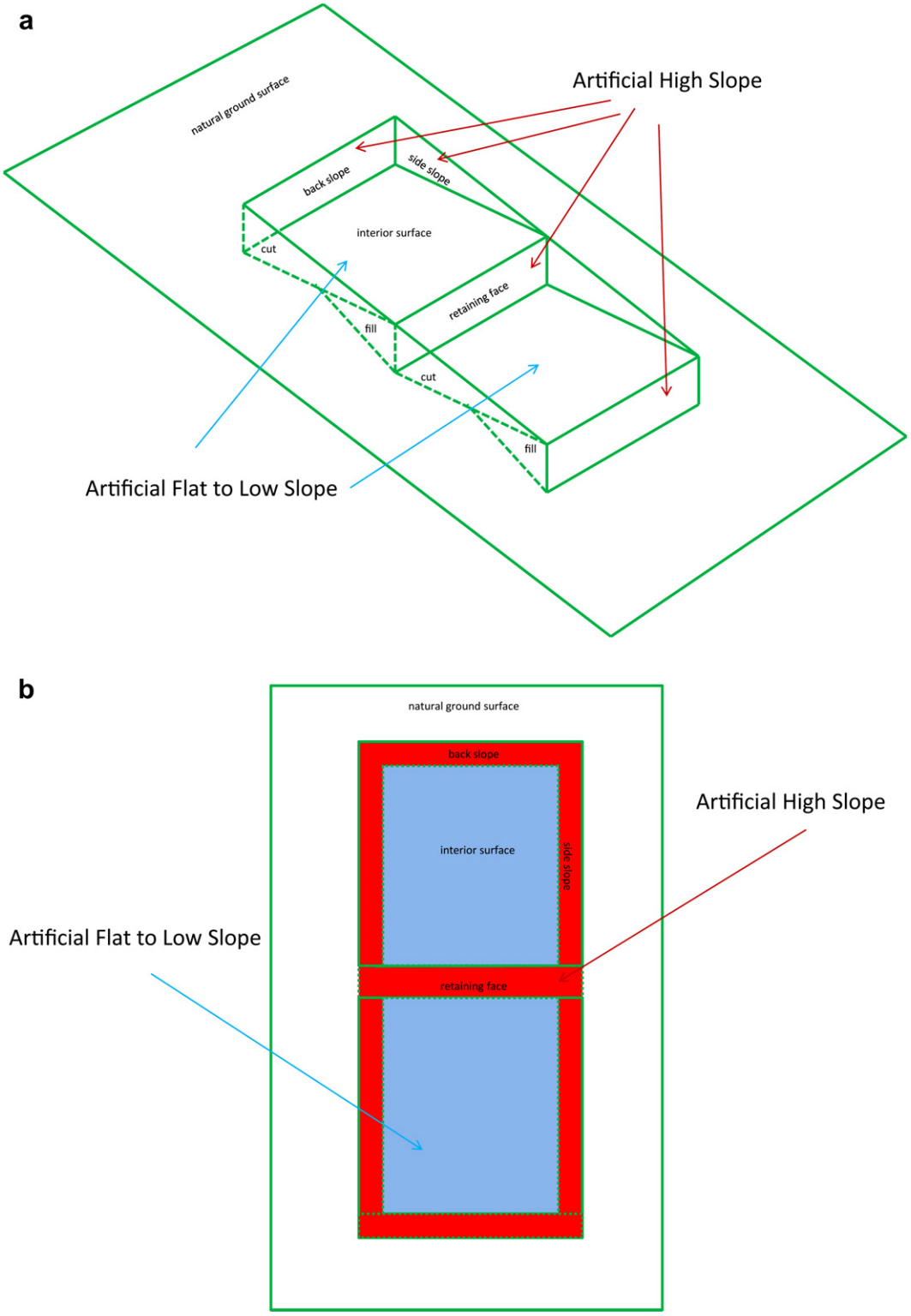

Fig. 4. Diagram of terrace. Note the 'ringing' pattern that artificially high slope cuts and banks make around the flat interior of the features.

streams are known to carry enough water to irrigate many times the amount of valley bottom available for farming (Fig. 3). This is not to say that irrigation never failed, or that there weren't places in the valley bottoms where irrigation failed to reach. The important point is that generally rainfall and stream flow do not appear to be critical limiting factors of taro cultivation in the study area. Nonetheless, a more detailed hydrological model would be valuable in determining how this system worked in practice.

The other factor to consider is the capability of irrigation systems to transport sufficient amounts of water to sustain irrigated fields outside of drainages. Hawaiian canals, called '*auwai*, are generally quite small and have only rarely been documented moving water outside of a natural drainage. Fortunately, in 2008 we exposed a series of canals in cross-section associated with a small group of valley fields. The few intact portions of these canals on the surface and the natural contour of the land led us to believe they were part of an effort to bring water to the east of the drainage. For this paper, we reconsidered these canals to determine how effective they were as water delivery systems and then compare the results to the amount of tableland available as determined through slope contrast mapping.

3. Methods

3.1. Lidar data collection and DEM

We used the Carnegie Airborne Observatory (CAO; Asner et al., 2007) to collect lidar data for the North Kohala area in January 2009. The CAO lidar was operated at 50 kHz, with a maximum half-scan angle of 17° (after 2-degree cutoff) and 35–40% overlap between adjacent flightlines. Sensor to ground range was maintained at 2000 m with a standard deviation of 90 m throughout the data collection. This resulted in +4.6% variation in laser ranging at the edge of each scan line, and +6 cm variation in laser spot spacing. Laser spot size at ground level ranged from 1.21 to 1.33 m from nadir to the edge of each scan line (17° off-nadir).

From the lidar point cloud data, a physically-based model was used to estimate top-of-canopy and ground DEMs using REALM (Optech Inc., Toronto, Canada) and TerraScan/TerraMatch (Terrasolid Ltd., Jyväskylä, Finland) software packages. Vertical errors in ground heights and vegetation heights were previously estimated to be 0.12 m (s.e. = 0.14 m) and 0.7 m (s.e. = 0.2 m), respectively, in a sub-set of a forest study that included both sloping and flat

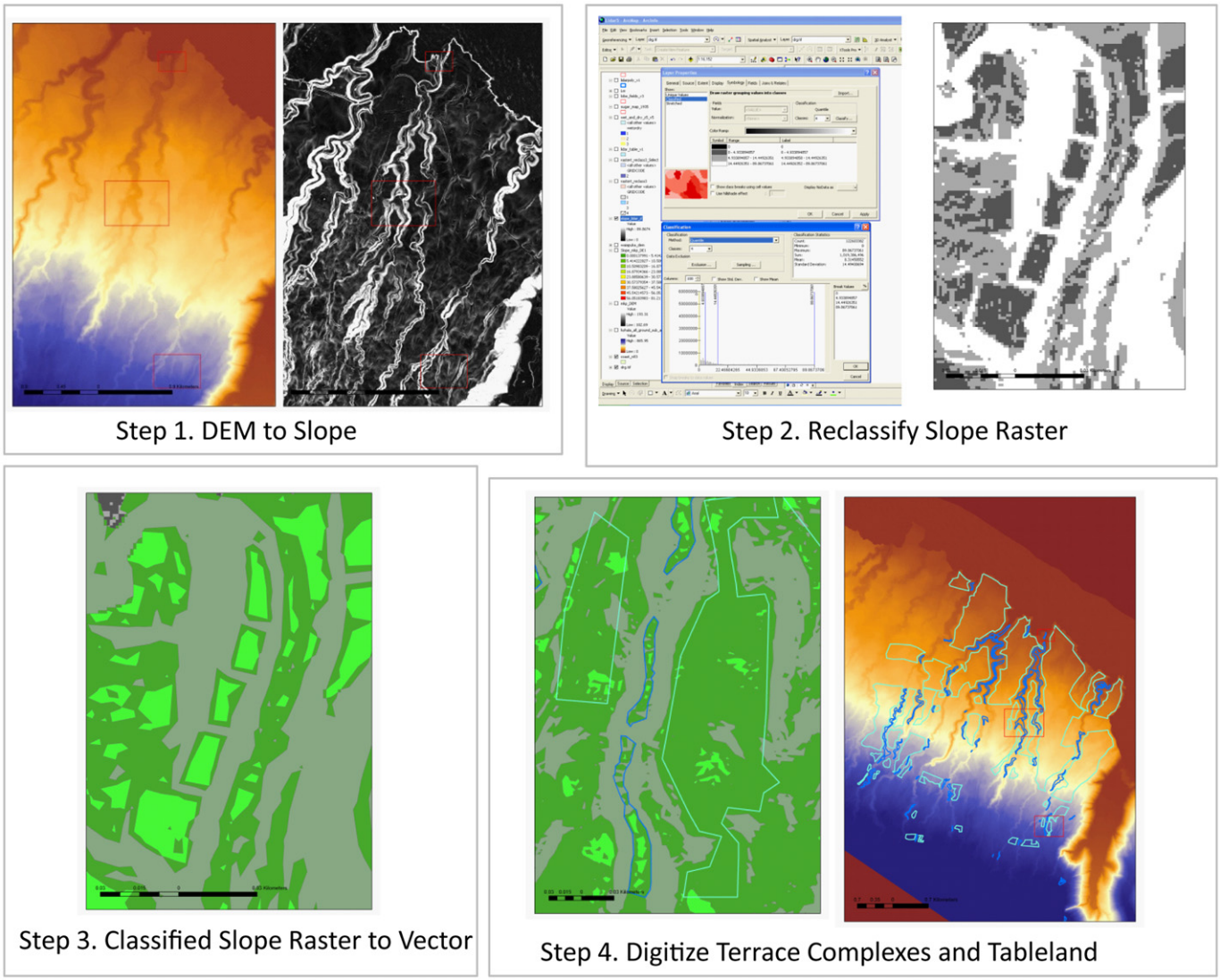

Fig. 5. Slope Contrast Mapping Method. See text for description of stages.

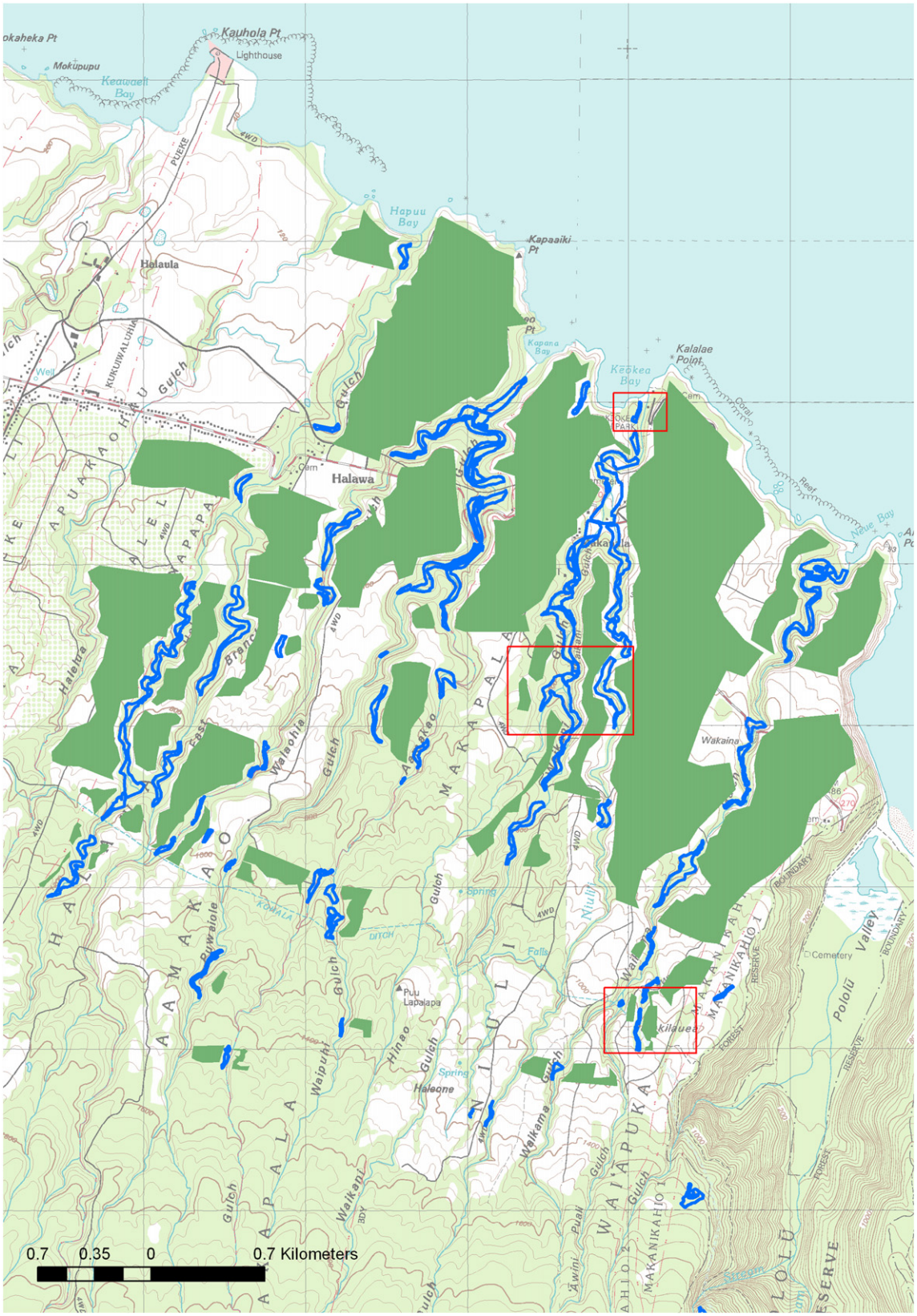

Fig. 6. Irrigation Complexes and Tableland Identified through Slope Contrast Mapping. Locations of detailed study areas are shown, from north to south: Niuli'i, Makapala, and Waiapuka.

terrain, with and without tree cover (Asner et al., 2007, 2008). A total of 6612 ha were flown at 1.12 m laser spot spacing.

Naturally, a higher density of lasers is always possible with lower altitude flights, for example Sittler (2010) and Chase et al. (2011) report on a datasets flown at 1000 and 800 m, respectively. We chose the survey parameters described here in order to efficiently cover a large area, including a large portion of the Kohala Mountains not reported here.

3.2. GIS methodology for slope contrast mapping

To increase our chances of recognizing terraces we began by developing a clear conceptual model of what typical terrace should look like in a slope contrast map. As shown in Fig. 4, a typical terrace changes the natural slope in two ways. Cutting and filling creates an artificially steep, often vertical, slope around the feature. In the hypothetical example shown here, the vertical back slope of 90° is created by a cut out of a natural slope. Side slopes (also 90°) are built from a combination of cutting and filling, and the downslope is composed of fill held in place by a retaining face. Naturally, the point of this earthmoving and construction is the creation of an artificially flat surface (0° slope). In the case of agricultural terraces used as pondfields, the interior must be as flat as possible to impound water behind a ringing bund made of earth, or earth and stone. While these bunds rarely survive, the use of stone for retaining walls helps these features stay intact for centuries. For example, near Hapu'u Bay we have recorded a stone terrace that was built up by a series of additional courses of stone and interior fill laid down over an estimated 700 years (McCoy et al., 2010:Fig. 2) (Fig. 5).

3.2.1. Step 1. Transform DEM to slope raster

First, the DEM was transformed in ArcGIS 9.3.1 (ESRI, Redlands, California) to a slope raster with the same resolution. This standard function calculates slope by searching in a 3 × 3 cell matrix for elevation change and assigns slope values as degrees or percent slope. In this case, we used degrees and not surprisingly our derived slope layer had values ranging from flat (0°) to near vertical (89.9°).

3.2.2. Step 2. Classify slope raster by flat, low slope, and high slope regions

The next step was to turn the slope raster in to a 'classified' raster by categorizing cells into three classes: flat, low slope, and high slope. To determine the break values for these we arrived at the quantile classification method as the most heuristic. In the quantile classification method, each class contains an equal number of cells. So, in effect, this presumes that the landscape is a third flat, a third low slope, and a third slope and produces the following ranges: flat = 0–4.93°; low slope = 4.93–14.45°; high slope = 14 to maximum slope, 89.87°.

Trial-and-error suggests that to produce a useful classification scheme (i.e., one that shows the contrast between natural and cultural features), it is important to use as few classes as necessary and identify values that will mask variation within key anatomical features of terraces. For example, while the natural slope of streams in the study area falls within the same ranges as terrace interiors (flat-to-low slope), archaeological features are distinct in their uniquely 'ringed' shape created by virtue of being surrounded by higher slope banks. Further, a terrace's retaining faces, while sometimes in the same high slope classification as a background high natural slope nonetheless show clear breaks between features.

3.2.3. Step 3. Transform classified slope raster to vector polygon layer

The classified slope raster alone could be used to create a contrast map; however, we found that transformation to vector polygons is extremely useful for grouping similar areas together. The lidar DEM has inherent roughness from low ground vegetation and stones and the GIS search pattern used in calculating slope creates patchy, higher than expected slope values within areas that would otherwise be considered flat. However, it is possible to mask this micro-variation by converting the classified raster to a vector layer; a process that filters anomalous, isolated cells when defining continuous areas.

3.2.4. Step 4. Digitize targeted archaeological and natural features

The last step involved digitizing the outlines of terrace complexes and tablelands. For the terrace complexes, the goal was to outline complete irrigation systems by prospecting along streams (Fig. 6). For tablelands, the goal was to use the boundary between flat tableland and valleys as breakline edges to define what areas immediately adjacent to valley fields could have been watered. The search pattern was similar to prospecting for valley fields. To be conservative about how far these systems could expand, we avoided delineating areas downslope of valley fields that could only have been reached through long canals (+100 m) and/or secondary flow between tableland fields.

3.3. Method for estimating area of tableland irrigated using canals

Here we reconsidered canals found in excavations to determine how effective they might have been as water delivery systems. We built upon a classic study of prehistoric irrigation canals constructed by the Hohokam of Southern Arizona (Busch et al., 1976), in which flow was calculated based on velocity and area, or $Q = A^*V$, where Q is flow in cubic meters per second (m^3/s), A is area of the flow cross-section (m^2), and V is the mean velocity in meters per second (m/s). While a canal's cross-section area is easily derived from our trench profile, we had to make several assumptions to determine velocity based on Manning's Equation, $V = (1/N)\, R^{2/3}\, S^{1/2}$, a formula commonly used for open channel hydraulics. N is a constant determined by empirical measurements of how the roughness of a surface impedes flow. Here we used 0.27, a value appropriate for earth canals. R is the hydraulic radius, which was calculated as area (m^2) over the wetted perimeter (m). S is slope of the canal expressed as a decimal. Since we do not have complete canals to determine this value empirically we used an average found for Hohokam canals, 1.89 m per kilometer ($S = 0.00189$). This is an extremely gentle grade relative to the natural landscape in the study area and thus represents a conservative estimate for velocity. Finally, once flow (Q) was calculated it was then divided by the Hawaiian Legal Requirement (280,000 L per day per hectare) to determine the amount of area (hectare) that could have been irrigated by the canals exposed by our excavations.

Table 1
Estimated Irrigated Valley Fields by Watershed.

	Historic Era Agriculture[a]		GIS Model Agriculture[b]		Lidar Agriculture	
	n	ha	n	ha	n	ha
Hapu'u	9	7.9	29	22.9	19	12.4
Kapanaia	18	11.3	73	28.9	49	20.6
Keokea	25	12.1	28	33.2	30	22.3
Neue	2	1.0	28	9.5	22	9.7
	54	32.3	158	94.5	120	65.0

[a] Data from McCoy and Graves (2010), lower than previous estimate due to tableland fields removed from calculation.
[b] Data from Ladefoged et al., (2009).

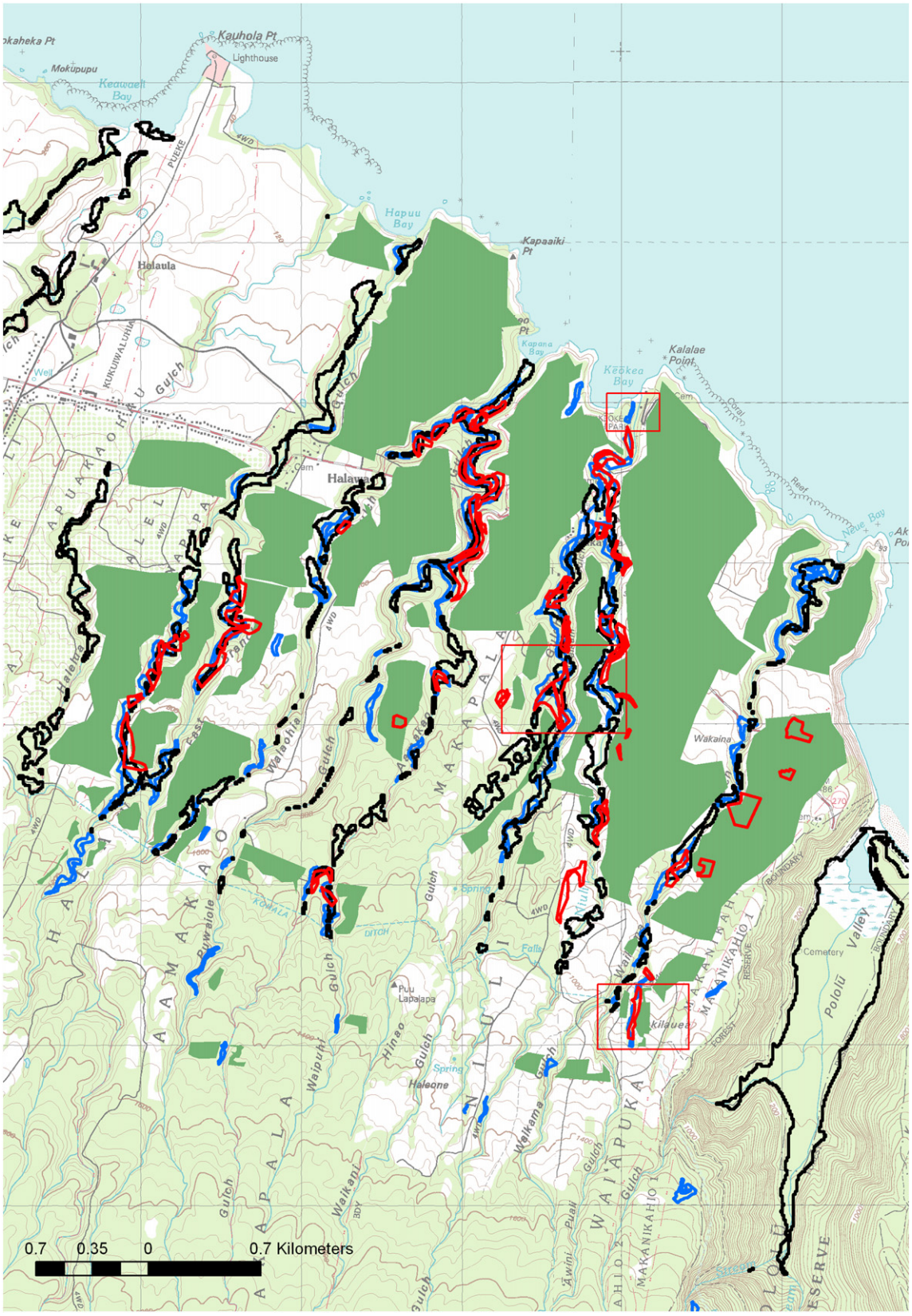

Fig. 7. Comparison of Historic, GIS Model, and Slope Contrast Maps of Complexes.

4. Results of slope contrast mapping archaeological and natural features

4.1. Mapping irrigation complexes within small valleys

Two previous attempts have been made to quantify the peak total area cultivated in the small valleys of the eastern Kohala District. A minimum area cultivated has been estimated digitizing historic maps (McCoy and Graves, 2010), hereafter referred to as the historic dataset, which resulted in a total area of 32 ha, including the few irrigated fields that still remained at the turn of the century. Ladefoged et al. (2009) used a course grained DEM and environmental data (elevation as proxy for rainfall, geological substrate age), hereafter referred to as the GIS model, to estimate the total amount of arable land for irrigation and came up with 94 ha.

Slope contrast mapping identified a total of 65 ha within small valleys (Table 1). This lidar based evaluation includes about twice as much area as recorded on historic maps but still significantly less than the GIS model. Fig. 7 shows these three estimates together: historic model (red), the GIS model (black), and slope contrast mapping (blue). Within the lower elevations near the coast, there is relatively good agreement along streams, however in the uplands

Fig. 8. Field and Slope Contrast Maps of Niuli'i Detailed Study.

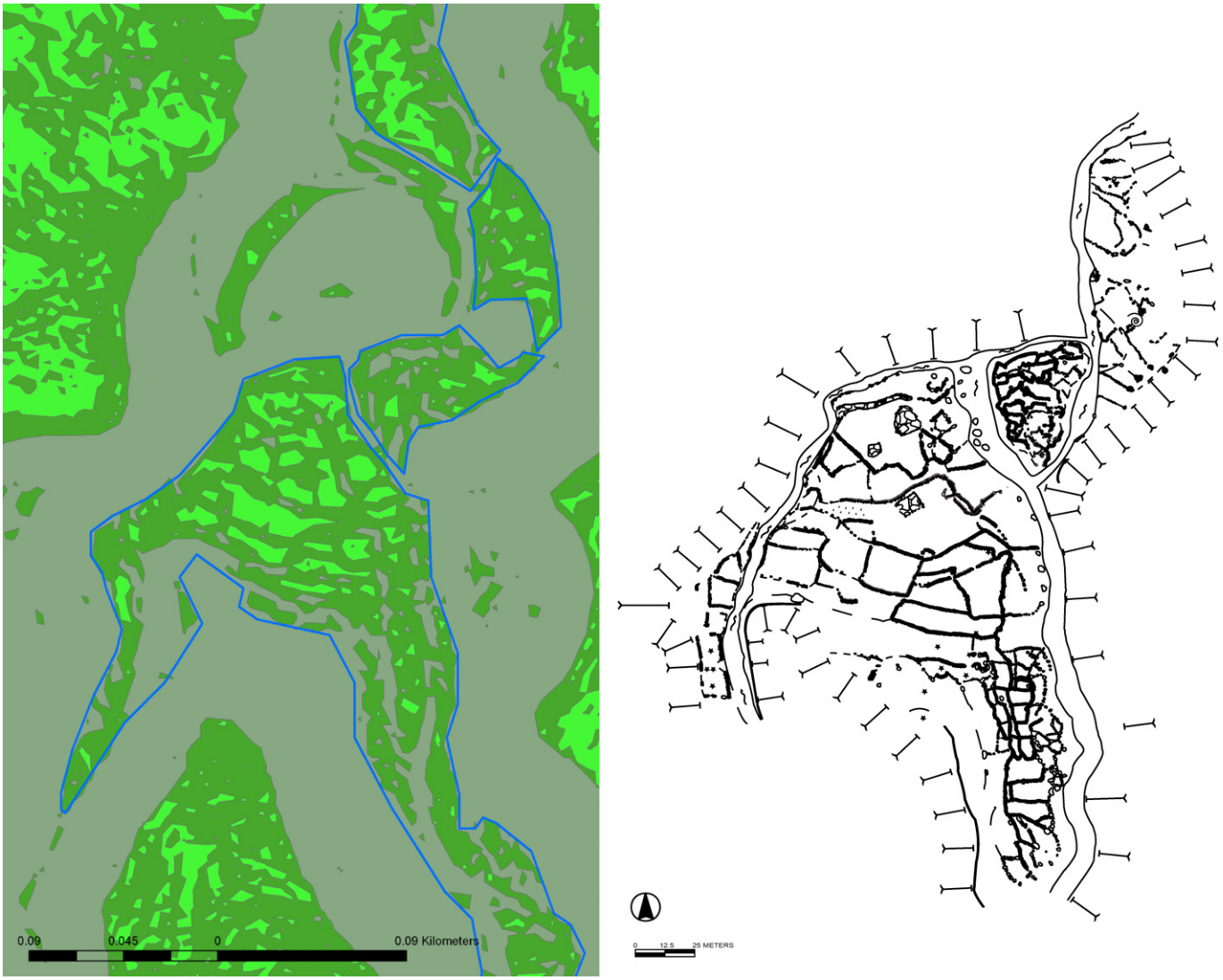

Fig. 9. Field and Slope Contrast Maps of Makapala Detailed Study Area.

the lidar model diverges in that it identifies a few fields at elevation beyond historic maps or the GIS model.

4.1.1. Detailed study areas: Niuli'i, Makapala, and Waiapuka

Next, we compared the new lidar datasets to our field survey data in three detailed study areas in terms of complex size and number terraces. In Niuli'i (NIU-1), field mapping recorded a small complex made up of 5 terraces in single row. Fig. 8 shows a lidar-derived DEM with slope contrast polygons compared with a survey map. In this case, the features have high contrast with the natural slope, are in good condition, and while there are mature trees throughout, the features are generally clear of understory. Lidar clearly matches well in both the size and number of features.

In Makapala (MKP-1, -2, and -3), the conditions for field survey and lidar based contrast mapping were significantly more difficult with thick understory as well as a mature overstory (Fig. 9). Nonetheless, there is again agreement in the size of the complexes as recorded on survey and slope contrast mapping. There is however a marked difference in the number of features recorded, with small terraces represented poorly in the slope contrast map.

In Waiapuka (WAI-4W), vegetation is again thick, but the complex is located in a shallow gully with little overstory (Fig. 10). Again there is good agreement in the overall size of the complex, but in this case small terraces are well represented on the slope contrast map. However, what is far more important for this study is how the mapping of adjacent tablelands relates to the expected size of fields based on canal capacity.

4.2. Mapping natural areas suited for tableland agriculture

Defining the limits of expansion of irrigated farming is important to developing a clear picture of the traditional Hawaiian political economy in the Kohala District. Fig. 6 shows the maximum area identified as appropriate tableland for irrigation (i.e., relatively flat, located adjacent to valley fields). While it is unlikely that all 688 ha of this region was indeed irrigated, slope contrast mapping made it possible to calculate this maximum area by defining the edges of small valleys not otherwise shown on maps of the region.

4.2.1. Comparing canal capacity and amount of available tableland for irrigation

To answer the question of how well our lidar-derived estimates of available tableland compared with the capacity of canals to carry irrigation water to these areas, we return to consider the excavation

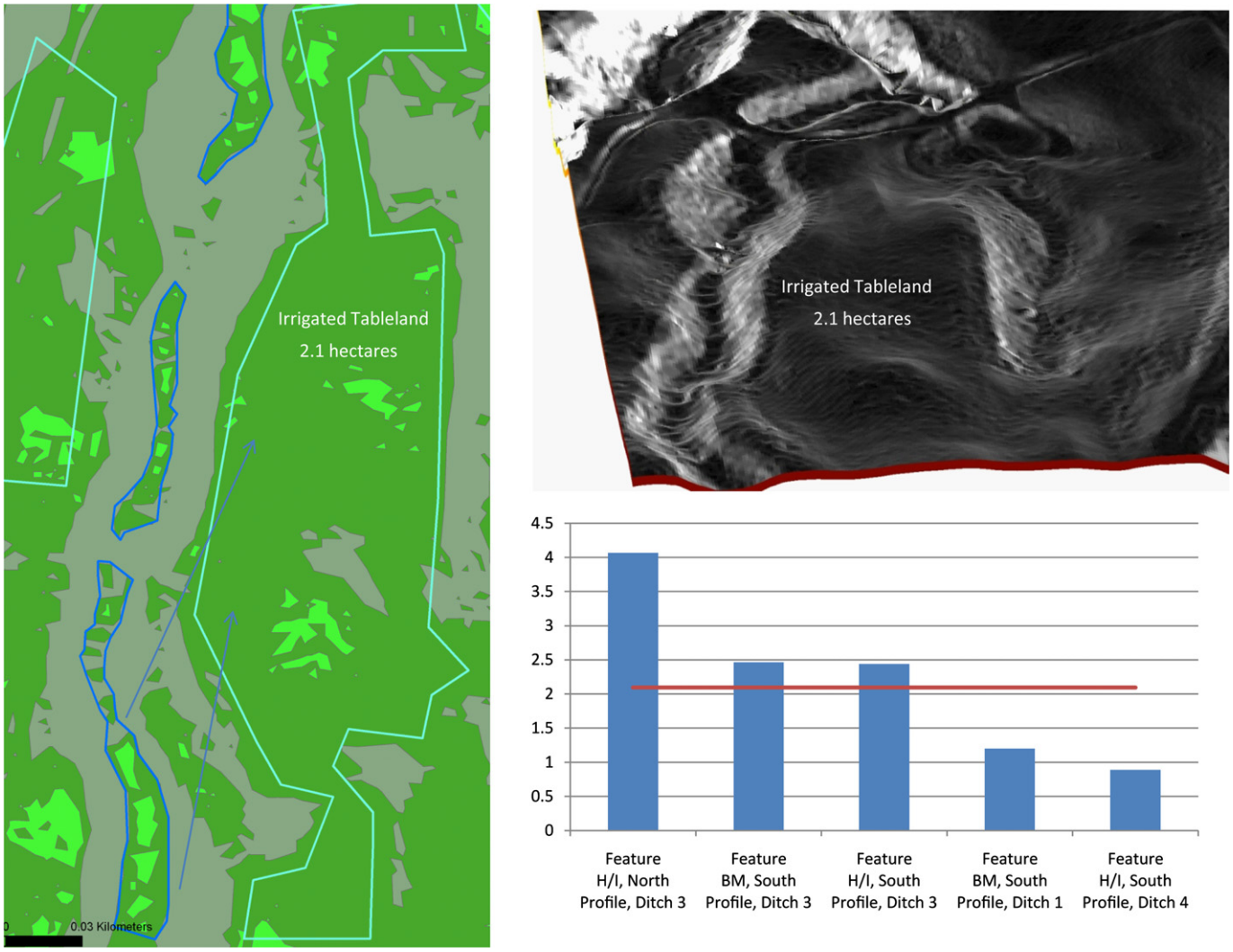

Fig. 10. Comparison of estimated canal irrigation capacity and available tableland in detailed study area of Waiapuka (WAI-4W). Note modern road in background.

data from Waiapuka. Based on cross-sections of cannels, we find capacity in three size classes (1, 2, and 4 ha) with an average of 2.3 ha (Fig. 10; Table 2). If this data corresponds to distinctly different sized canals, then the smaller sized ones would have watered about 1 ha worth of taro, the mid-sized around 2 ha, and the largest around 4 ha. If we compare these estimates to the few fields that survived to the turn of the century, the smaller size range matches the range observed for most fields, between 1.2 and 0.2 ha. The largest tableland fields in operation at the turn of the century, which was fed by an elaborate canal called Kamehameha's Tunnel, were 2.5 ha – close to the average size estimated here. However, no tableland fields survived to the historic period that would have been equal to the largest sized canal.

What seems more likely than the three size classes corresponding to different sized canals is the notion that these capacity measurements represent a range of variation within canals which were slightly differently sized along their courses. In fact where we were able to find good cross-sections of the same canal in two profiles (Feature H/I, Ditch 3), our estimates, 4 ha and 2 ha, clearly did not match. Therefore, we believe that the figure of 2.3 ha is probably close to the maximum area watered by these canals.

Table 2
Calculating Capacity of Canals. This table gives values used to calculate the total maximum area a canal could irrigate given its size and amount of flow necessary to grow taro (Hawaiian Legal Requirement). Note: Wetted perimeter and area were calculated from digitized excavation profiles (McCoy and Graves, 2008).

WAI_4W	Area (m^2)	Wetted Perimeter (m)	Hydraulic Radius (R = area/wetted perimeter)	Roughness	Line Slope	Velocity of Flow (m/sec)	Velocity of Flow (Q) (m^3)	Equivalent Irrigated Area (ha)
Feature H/I, North Profile, Ditch 3	0.044422	0.583	0.076196	0.027	0.00189	0.292881	0.01301	4.1
Feature BM, South Profile, Ditch 3	0.029801	0.455612	0.065409	0.027	0.00189	0.264812	0.007892	2.5
Feature H/I, South Profile, Ditch 3	0.029956	0.469	0.063872	0.027	0.00189	0.26069	0.007809	2.4
Feature BM, South Profile, Ditch 1	0.017297	0.345	0.050136	0.027	0.00189	0.222187	0.003843	1.2
Feature H/I, South Profile, Ditch 4	0.013801	0.308935	0.044673	0.027	0.00189	0.205896	0.002842	0.89

As shown in Fig. 10, our lidar DEM derived slope contrast map indicates 2.1 ha of tableland land would have been available for farming in the area downslope of these canals. While we find canals appear to have the capacity to water full-time an average of 2.3 ha these results are encouraging in that our methods of estimating maximum available tableland based on lidar and average capacity for irrigation based on canals have returned remarkably similar results.

5. Discussion

Developments in remote sensing are changing how archaeologists study the history of irrigation (e.g., Harrower, 2008). Mapping agricultural terrace complexes using lidar confirms the notion that windward North Kohala was a major region of irrigated agriculture. But, as in all archaeological prospection, slope contrast mapping has inherent methodological and interpretive limitations. Naturally, the first issue is determining when slope contrast mapping is appropriate when compared to the more typical hillshade approach. In this case, we knew our target features – artificial terraces and naturally flat tableland - were likely to be distinct from the rest of the landscape in terms of slope. Perhaps more importantly, we had survey data that allowed us to test several unsuccessful methods which we won't repeat in full here, but showed that hillshade proved ineffective in the detailed study areas where we knew well-preserved examples of terraces could be found. Sky-view factor also failed in this environment partially due to the fact that features are located in narrow valleys with uniformly limited views (Kokalj et al., 2011).

Probably the most critical issues in applying this approach are choosing appropriate break values in the slope classification process (Step 2) and the fact that interpreting results relies on the subjective identification of features through prospecting. Here we arrived at our break values through trail-and-error. But in other cases it might be necessary to undertake systematic experiments to arrive at the most effective break values. A triangulated irregular network (TIN) may also identify important breaklines without the need for slope contrast mapping. However, we found automated GIS breakline generation unfeasible especially compared with the flexibility slope contrast mapping allows in interpreting archaeological and natural features. Another challenge is the amount of computer processing power that it takes to classify and vectorize a detailed DEM derived from lidar data. There are obvious ways to avoid large file sizes such as geographically splitting the DEM one is working with. But with splitting there is the potential to introduce an edge effect and if break values are calculated on a sub-set of the DEM rather than standardized across the entire layer, then re-joining sub-regions could be problematic.

The discovery of 65 ha of intact small valley irrigated fields by lidar survey suggests the current GIS model of agricultural production (Ladefoged et al., 2009) is correct to attribute a substantial amount potential area for irrigated farming to the study area (94 ha), only a fraction of which are locatable on historic maps (32 ha). The GIS predictive model does not distinguish between potential areas of small valley farming and adjacent tableland suitable for agriculture, thus more research is necessary to scale the results here to the larger archipelago model. However, if for example the intact small valley fields described here are a good representation of the total maximum area farmed on Hawai'i Island (14 sq km; Ladefoged et al., 2009:Table 2), then the current GIS estimate is too high and might be better revised to near 10 sq km. But, if the now destroyed tableland fields played a significant role in production, then the current estimate could possibly be a gross underestimation.

What does this uncertainty in estimates of the peak amount of irrigated land under production mean for interpretations of the past? More than simply a numbers game, this issue is fundamental to how we model the development of the Hawaiian political economy and shapes how we see conditions on Hawai'i Island. For example, Graves et al.'s (2011) recent comparison of Hawai'i and Maui Island oral traditions indicates differences in their internal trajectories of territorial integration, political aggression, and elite marriage alliances can be seen to correlate with the distribution of different types and amounts of agricultural lands. Specifically, the somewhat greater balance between total amounts of productive land across Maui Island's districts, when compared to Hawai'i Island, may have promoted a more stable island-wide polity, as opposed to the frequent intra-island competition and conflict observed in Hawai'i Island traditions of the same era. It is only through a clear picture of the geographic extent and history of irrigated farming that we will be able to test this model and address the large question of why an archaic state society arose in Hawai'i.

6. Conclusions

Here we presented a case study where terrace complexes used for irrigated agriculture were located within small valleys using airborne lidar data. Slope contrast mapping also helped map naturally flat areas called tableland and thus defining where irrigated agriculture could have expanded in the past. The current GIS model of agricultural production in the Hawaiian Islands (Ladefoged et al., 2009), is correct to attribute a substantial amount potential area for irrigated farming to the study area, only a fraction of which are locatable on historic maps. However, future research should be aimed at determining the agricultural potential of small valley and tableland environments and how revisions to agricultural productivity impact our interpretations of trajectories of social change in the Hawaiian archipelago.

Acknowledgments

This research was supported by two grants from the National Science Foundation (Award SES-0552977 and BCS-0624238) and we would like to recognize and thank our colleagues on these projects: Oliver Chadwick, Julie Field, Pat Kirch, Thegn Ladefoged, and Peter Vitousek. Special thanks to the staff of the CAO for all their help, especially Ty Kennedy-Bowdoin. Surety Kohala Corporation, Kamehameha Schools, Vipassana Hawai'i, New Moon Foundation and George and Alexa Russell graciously granted us permission to conduct archaeological research on their property. This paper was originally presented at the 2010 Society for American Archaeology meetings and we would like to again thank the session's organizer, Jennifer Campbell, and all those who attended and offered helpful comments. Thanks also to Thegn Ladefoged, Peter Vitousek, and anonymous reviewers who helped improve this paper with their comments.

References

Asner, G.P., Knapp, D.E., Jones, M.O., Kennedy-Bowdoin, T., Martin, R.E., Boardman, J., Field, C.B., 2007. Carnegie airborne observatory: in-flight fusion of hyperspectral imaging and waveform light detection and ranging for three-dimensional studies of ecosystems. Journal of Applied Remote Sensing 1. doi:10.1117/1.2794018.

Asner, G.P., Hughes, R.F., Vitousek, P.M., Knapp, D.E., Kennedy-Bowdoin, T., Boardman, J., Martin, R.E., Eastwood, M., Green, R.O., 2008. Invasive plants alter 3-D structure of rainforests. Proceedings of the National Academy of Sciences 105, 4519–4523.

Bewley, R.H., Crutchley, S.P., Shell, C.A., 2005. New light on an ancient landscape: lidar survey in the Stonehenge world heritage site. Antiquity 79, 636–647.

Brown, A.G., 2008. Geoarchaeology, the four dimensional (4D) fluvial matrix and climatic causality. Geomorphology 101, 278–297.
Busch, C.D., Raab, L.M., Busch, R.C., 1976. Q = A × V: prehistoric water canals in Southern Arizona. American Antiquity 41, 531–534.
Campbell, J.B., 2007. Introduction to Remote Sensing, Forth Ed. Guilford Press, New York.
Carey, C.J., Brown, T.G., Challis, K.C., Howard, A.J., Cooper, L., 2006. Predictive modelling of multiperiod geoarchaeological resources at a river confluence: a case study from the Trent-Soar, UK. Archaeological Prospection 13, 241–250.
Chase, A.F., Chase, D.Z., Weishampel, J.F., 2010. Lasers in the Jungle. Archaeology Magazine, vol. 63. http://www.archaeology.org/1007/etc/caracol.html (accessed 26.07.10.).
Chase, A.F., Chase, D.Z., Weishampel, J.F., Drake, J.B., Shrestha, R.L., Slatton, K.C., Awe, J.J., Carter, W.E., 2011. Airborne LiDAR, archaeology, and the ancient Maya landscape at Caracol, Belize. Journal of Archaeological Science 38, 387–398.
Challis, K., 2006. Airborne laser altimetry in alluviated landscapes. Archaeological Prospection 13, 103–127.
Challis, K., Carey, C., Kincey, M., Howard, A.J., 2011. Assessing the preservation potential of temperate, lowland alluvial sediments using airborne lidar intensity. Journal of Archaeological Science 38, 301–311.
Challis, K., Kokalj, Z., Kincey, M., Moscrop, D., Howard, A.J., 2008. Airborne lidar and historic environment records. Antiquity 82, 1055–1064.
Challis, K., Howard, A.J., 2006. A review of trends within archaeological remote sensing in alluvial environments. Archaeological Prospection 13, 231–240.
Coluzzi, R., Masini, N., Lasaponara, R., 2011. Flights into the past: full-waveform airborne laser scanning data for archaeological investigation. Journal of Archaeological Science 38, 2061–2070.
Crow, P., Benham, S., Devereux, B.J., Amable, G.S., 2007. Woodland vegetation and its implications for archaeological survey using LiDAR. Forestry 80, 241–252.
Crutchley, S., 2006. Light detection and ranging (lidar) in the Witham Valley, Lincolnshire: an assessment of new remote sensing techniques. Archaeological Prospection 13, 251–257.
Devereux, B.J., Amable, G.S., Crow, P., Cliff, A.D., 2005. The potential of airborne lidar for detection of archaeological features under woodland canopies. Antiquity 79, 648–660.
Doneus, M., Briese, C., Fera, M., Janner, M., 2008. Archaeological prospection of forested areas using full-waveform airborne laser scanning. Journal of Archaeological Science 35, 882–893.
Earle, T.K., 1980. Prehistoric irrigation in the Hawaiian Islands: an evaluation of evolutionary significance. Archaeology and Physical Anthropology in Oceania 15, 1–28.
Earle, T.K., 2002. Bronze Age Economics: The Beginning of Political Economies. Westview Press, Cambridge, Mass.
Gallagher, J.M., Josephs, R.L., 2008. Using LiDAR to detect cultural resources in a forested environment: an example from Isle Royale National Park, Michigan, USA. Archaeological Prospection 15, 187–206.
Graves, M.W., Cachola-Abad, C.K., Ladefoged, T.N., 2011. The evolutionary ecology of Hawaiian political complexity: case studies from Maui and Hawai'i island. In: Kirch, P.V. (Ed.), Roots of conflict: soils, agriculture, and sociopolitical complexity in ancient Hawaii. Advanced Seminar Series. School for Advanced Research Press, Santa Fe, New Mexico.
Harmon, J.M., Leone, M.P., Prince, S.D., Snyder, M., 2006. Lidar for archaeological landscape analysis: a case study of two eighteenth-century Maryland plantation sites. American Antiquity 71, 649–670.
Harrower, M.J., 2008. Hydrology, ideology, and the origins of irrigation in ancient Southwest Arabia. Current Anthropology, 497–510.
Hesse, R., 2010. LiDAR-derived local relief models – a new tool for archaeological prospection. Archaeological Prospection 17, 67–72.
Kirch, P.V., 1994. The Wet and the Dry: Irrigation and Intensification in Polynesia. University of Chicago, Chicago.
Kirch, P.V., 2010. How Chiefs Became Kings. University of California Press, Berkeley.
Kirch, P.V., McCoy, M.D., 2007. Reconfiguring the Hawaiian cultural sequence: results of re-dating the Halawa Dune site (MO-A1-3), Molokai island. Journal of the Polynesian Society 116, 385–406.
Kokalj, Z., Zaksek, K., Ostir, K., 2011. Application of sky-view factor for the visualisation of historic landscape features in lidar-derived relief models. Antiquity 85, 263–273.
Ladefoged, T.N., Kirch, P.V., Gon III, S.O., Chadwick, O.A., Hartshorn, A.S., Vitousek, P.M., 2009. Opportunities and constraints for intensive agriculture in the Hawaiian Archipelago prior to European Contact. Journal of Archaeological Science 36, 2374–2383.
Lasaponara, R., Coluzzi, R., Gizzi, F.T., Masini, N., 2010. On the LiDAR contribution for the archaeological and geomorphological study of a deserted medieval village in Southern Italy. Journal of Geophysics and Engineering 7, 155–163.
McCoy, M.D., Graves, M.W., 2007. An Archaeological Survey of Halawa and Makapala Ahupua'a, North Kohala District, Hawai'i Island: Hawai'i Archaeological Research Project 2007. Report on file with the Hawaii State Historic Preservation Division, Kapolei.
McCoy, M.D., Graves, M.W., 2008. An Archaeological Investigation of Halawa and Waiapuka Ahupua'a, North Kohala District, Hawai'i Island. Report on file with the Hawaii State Historic Preservation Division, Kapolei.
McCoy, M.D., Graves, M.W., 2010. The role of agricultural innovation on Pacific Islands: a case study from Hawai'i Island. World Archaeology 42, 90–107.
McCoy, M.D., Graves, M.W., Murakami, G., 2010. The Introduction of breadfruit (*Artocarpus altilis*) to the Hawaiian islands. Economic Botany 64, 374–381.
McCoy, M.D., Ladefoged, T.N., 2009. New developments in the use of spatial technology in archaeology. Journal of Archaeological Research 17, 263–295.
Millard, K., Burke, C., Stiff, D., Redden, A., 2009. Detection of a low-relief 18th-century British siege trench using LiDAR vegetation penetration capabilities at Fort Beausejour-Fort Cumberland National historic site, Canada. Geoarchaeology: An International Journal 24, 576–587.
Parcak, S., 2009. Satellite Remote Sensing for Archaeology. Routledge, Oxon, U.K.
Rowlands, A., Sarris, A., 2007. Detection of exposed and subsurface archaeological remains using multi-sensor remote sensing. Journal of Archaeological Science 34, 795–803.
Sittler, B., 2010. Revealing historical landscapes by using airborne laser scanning: a 3-D model of ridge and furrow in forests near Rastatt (Germany). In: Kolbe, T.H., Koing, G., Nagel, C. (Eds.), 5th International Conference on 3D GeoInformation. Institute of Geodesy and Geoinformation Science, Technische Universitat Berlin, Berlin, Germany. http://www.isprs.org/proceedings/XXXVI/8-W2/SITTLER.pdf.